ACADEMIA ROMÂNĂ
Revue Roumaine de Chimie
https://www.icf.ro/rrch/

Rev. Roum. Chim.,
2023, *68*(1–2), 5–16
DOI: 10.33224/rrch.2023.68.1-2.01

KINETICS OF PHOSPHATE ADSORPTION FROM AQUEOUS SOLUTION INTO ORGANOBENTONITE BY CATIONIC POLYMER GRAFTED BENTONITE

Moussa AMRANI[a,*] and Samira BANDOU[a]

[a]Laboratory of Soft Technology, Recovering, and Sustainable Development Faculty of Science, M'Hamed Bougara University, BP 70, 35000 Boumerdes, Algeria

Received June 14, 2017

Natural clays are abundantly available low-cost natural resource which is nontoxic to ecosystem. Over the recent years, research on the modification of clay to increase their adsorbent capacity to remove contaminants from aqueous solution. In this study, natural bentonite was modified with polydimethyldiallil tetraammonium chloride (PDMDMAC) and Hexadecyltrimethylammonium bromide (HDTMAB). Bentonite, PDMDMA-Bt and HDTMA-Bt were then characterized using XRD, XRF, SEM, FT-IR, elemental analysis and Brunauer-Emmett-Teller (BET) surface area techniques. The $HDTMA^+$ and $PDMDMA^+$ cations were found to be located on the surface and enters the interlayer spaces of smectite according to the XRD and SEM results. FT-IR spectra indicated the existence of HDTMA PDMDMA functional groups on the bentonite surface. The BET surface area significantly decreased after the modification due to the coverage of the pores of natural bentonite. After the characterization, the kinetics adsorption of phosphate ions ($PO4^{-3}$) onto betonies, HDTMAB-Bt and PDMDMA-Bt was investigated. On kinetic data representation, pseudo-first, pseudo-second order and intraparticle diffusion models were used, with the pseudo-second-order model gave better correlation, which indicates chemisorption between adsorbent and adsorbate molecules.

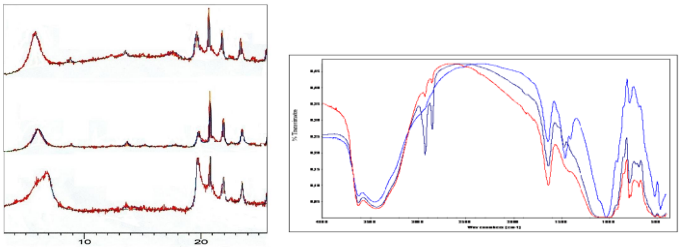

INTRODUCTION

Phosphorus is of central concern to a wide variety of biological and chemical processes in natural waters. An excessive concentration of phosphorus in water is often responsible for eutrophication leading to short- and long-term environmental and aesthetic problems in lakes and reservoirs, coastal areas, and other confined water bodies, and is a threat to ecological health. Algal blooms causing high economic damage in coastal oceans can be caused by phosphate run-off episode.[1,2] In recent years, in order to control or alleviate eutrophication, phosphorus in the wastewater must be treated and reduced to a low level prior to discharge into water bodies.

Many treatment methods for phosphorus removal – including chemical, biological and adsorption – have been developed.[3-6] Among them, chemical method is reliable and easy-operated, but high cost and secondary pollution caused by abundant production of sludge are its main shortcomings.[7] In contrast, biological treatment is low-cost and less secondary pollution, but its

* Corresponding author: moussaamrani@yahoo.fr

removal efficiency is highly inconsistent due to environmental factors such as temperature, pH, and so on.[8-11] Adsorption method, which has the advantages of the two above mentioned methods, is probably a better choice for phosphorus removal. Adsorption of phosphate onto particulate matter is an important process that affects significantly the mobility and bioavailability of phosphorus in natural environments. Adsorption processes such as fixed-bed filtration systems are effective for the removal of low concentrations of phosphorus in water.[12,13] Recently, polycation-modified bentonite was proved to be of high efficiency for anions removal.[13-20] Although organo-bentonites could have similar properties, at strong acidic conditions, organic species can be leached and enter the water system as pollutant while polycations have a much stronger affinity to bentonite and are not easily desorbed.

However, the goals of this study were to focus on the preparation of modified bentonite adsorbents by changing some of the bentonite properties for the enhancement of the anionic adsorption capacity of phosphate anions, and on the adsorption kinetics of phosphate onto polycation/bentonite. Organic-modified untreated and acid activated bentonites were prepared using polydimethyldiallil tetraammonium chloride (PDMDMAC) and Hexadecyltrimethylammonium bromide (HDTMAB).

The modified products were characterised using X-ray diffraction (XRD), Fourier transform infrared (FTIR) spectroscopy, scanning electron microscopy (SEM). The adsorption kinetics of phosphate was examined using the batch adsorption method.

RESULTS AND DISCUSSION

Structural characterization

Elementary chemical analysis by X-ray fluorescence (Table 1) shows that aluminum oxide (Al_2O_3) and silicon oxide (SiO_2) are the predominant constituents with a ratio SiO_2/Al_2O_3 equal to 2.47. This value and the low content of K_2O (0.65%) indicate that the clay used in this work belongs to the family of smectite. The presence of exchangeable cations such calcium (Ca^{2+}), sodium (Na^{+}) and magnesium (Mg^{2+}) indicates that the analyzed sample has a high cation exchange capacity. These results are completely consistent with those reported by B. Makhoukhi (2008)[23] for an Algerian bentonite.

Fig. 1 illustrates the XRD patterns (2θ values of 2–25°) for the Na-Bt, PDADMAC/Bt and HDTMAB/Bt materials. The examination of the positions of this XRD patterns suggests that this clay is predominantly composed of montmorillonite. The other peaks are impurities corresponding to quartz, mica, magnesite, feldspar and calcite. The d001 value of the peak in the XRD pattern of Na-Bt was 12,71Å (for 2θ = 7.22°), whereas PDADMAC/Bt increased this value to 14.55 Å (for 2θ= 5.66°), and HDTMAB/Bt modification caused an increase of 15.90 Å (for 2θ= 5.06°) is shown in Fig. 4. The results of XRD analysis reveal that basal spacings of PDADMAC/Bt and HDTMAB/Bt increase by 1.84Å and 3.19 Å, respectively. A shift of the d-spacing of the modified bentonites to lower diffraction angles when compared to the unmodified Na-Bt (Table 2). According to the model proposed by Lagaly and Weiss 1970,[24] a less than 18 Å increase in basal spacing corresponds to a mono layer formation on the surface. This observation suggests that the PDADMAC and HDTMAB grafted molecules, partially intercalated into interlayer's bentonite with monolecular layer.[25-27] The shape and width of a peak in a XRD pattern provide information about the homogeneity and structural differences of the modified products,[19] and broader peak widths indirectly indicate an early stage of disordered organic molecules in the interlayer space.[28] Therefore, the existence of smooth and narrow peaks in the XRD patterns for PDADMAC and HDTMAB products confirmed the creation of a new homogeneous structure in Bent.

Table 2 shows the surface area for the different samples. The specific surface areas of Na-Bt, PDADMAC /Bt and HDTMAB/Bt were 87.87, 18.35 and 13.88 m^2/g respectively. This result verified that internal surfaces of the Bentonite were filled with the organic surfactant and N_2 gas could not reach these internal surfaces. This decrease may also indicate surfactant loading on the clay surface, blocking a portion of the specific surface area, as given by Xi *et al.*[28] Moreover, intercalation of organic cations on bentonite may verify the formation of new porous structures and this provides highly efficient adsorption sites for anions Zhu and Zhu.[29] As seen in Table 2, the addition of the quaternary salt, PDADMAC and HDTMAB, to bentonite cannot exchange inorganic ions of bentonite interlayer completely, which could be attributed to the interface obstruction of polymer intercalation into bentonite layer s and the reversibility of exchange reaction.[30]

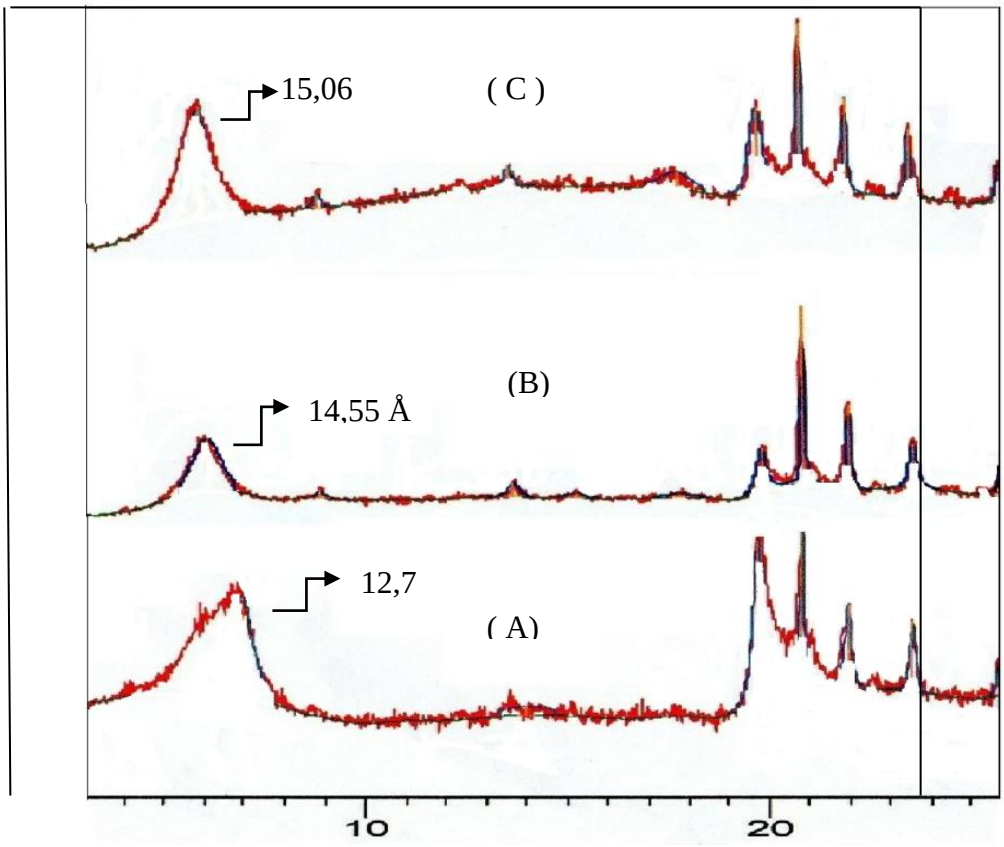

Fig. 1 – X-ray diffractions patterns of Na-Bt (A), PDADMAC/Bt (B) and HDTMAB/Bt (C).

Table 1

Main chemical composition of bentonite

Elemental oxides	wt (%)
SiO_2	**60.45**
Al_2O_3	**24.39**
Fe_2O_3	**0.79**
CaO	**1.10**
MgO	**2.60**
Na_2O	**2.88**
K_2O	**0.87**
LOI	**5.25**
SiO_2/Al_2O_3	**2.47**

LOI: Loss of ignition between 700–1000◦C

Table 2

Summary of XRD, CEC, and BET analysis results of Na-Bt, PDADMAC-Bt, and HDTMAB-Bt

Samples	BET, surface area (m^2/g)	d001 (A°)	2 θ
Na-Bt	87.87	12.71	6.89
HDTMAB/Bt	18.35	15.90	5.06
PDADMAC /Bt	13.88	14.55	5.66

FTIR measurements

FTIR spectra of Na-Bt, PDADMAC /Bt and HDTMAB/Bt are given in Fig. 2. At 3,600 cm^{-1} band, attributed to the valence vibration of the OH group, the peaks for both bentonite samples are the same. But within 2,000 to 3,000 cm^{-1} band region, the peaks are well pronounced on PDADMAC and

HDTMAB treated clay while such peaks are not found in Na-Bt spectra. Absorption bands assigned to antisymmetric and symmetric stretching vibrations of C-H were observed only on the modified bentonite spectrum at about 2,919 cm^{-1} and 2,838 cm^{-1}, respectively, indicating the presence of long alkyl chain in the bentonite.[31,32] These bands were less intense in PDADMAC than HDTMAB spectrum. The appearance of new bands around 1,662 cm^{-1}, which is the result of stretching vibrations of the C=O bond. The band at 2,851 cm^{-1} represents the general alkyl group (CH_3). The presence of CH_2 and CH_3 groups in the infrared spectrum of the treated samples is a good evidence of the intercalation of the ammonium quaternary cation of the surfactant within the interlamellar spaces of the sample.[22] A remarkable attenuation of the intensity of the bands at 1,610 cm^{-1} and 3,450 cm^{-1} relative to interlayer water was observed.[33] This attenuation increased with the initial surfactant amount surfactant loading. This result confirms the substitution of hydrated cations by those of HDTMA and PDADMAC[34] which is in perfect agreement with the literature.[35,36] A band at 1,450 cm^{-1} is assigned to the bending vibration of N-H groups,[37] indicated that HDTMA and PDADMAC have been grafted on Na-Bt.

Table 3

Interpretation of the FTIR spectra[21]

Wavelength (cm^{-1})	Attribution
3631	O-H, stretching of structural hydroxyls
3440	O-H, stretch of water molecules due to hydration
2926	Asymmetric CH_2 stretching
2852	Symmetric CH_2 Stretching
1643	O-H, bending of water molecules due to hydration
1089	Si-O stretching (also to cristobalite)
1035	Si-O, stretching (also to cristobalite)
915	Al-Al-OH, deformation
874	Al–Fe–OH bending
840	Al-Mg-OH, deformation
793	Cristobalite impurity
694	Presence of quartz
626	Al-O and Si-O out of the plane (also to cristobalite)
524	Al-O-Si, deformation
466	Si- O-Si, deformation

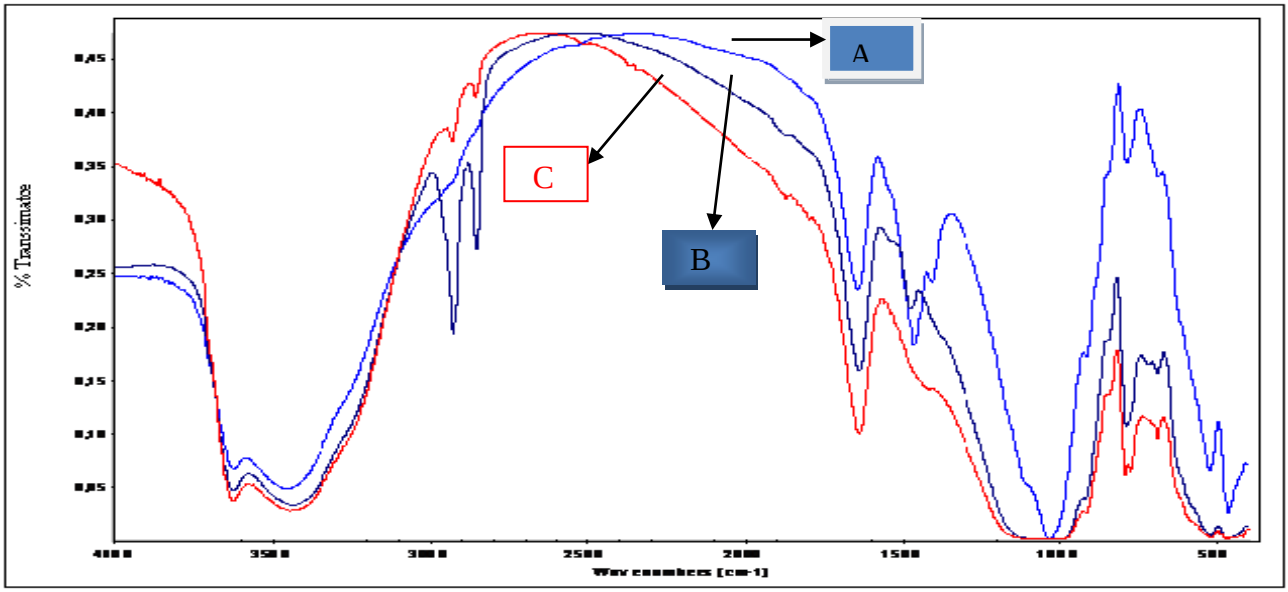

Fig. 2 – FT-IR spectrum of Na-Bt (A), PDADMAC-Bt (B), and HDTMAB-Bt (C).

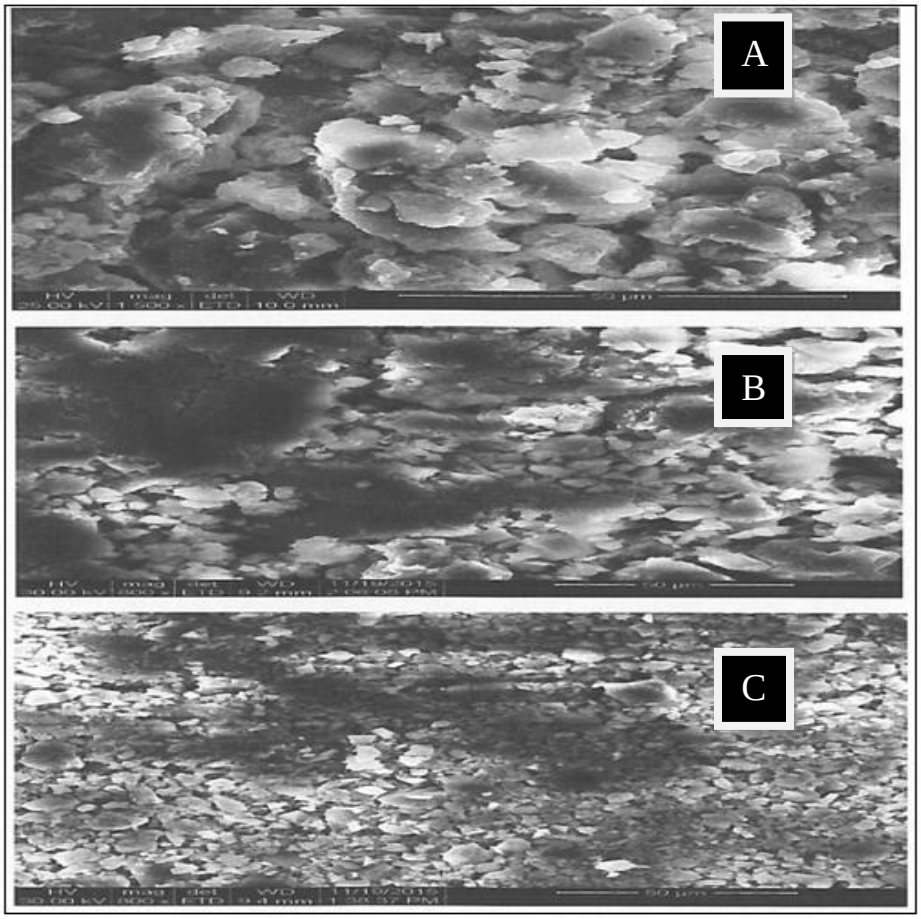

Fig. 3 – SEM images of Na-Bt (A), PDADMAC-Bt (B), and HDTMAB-Bt (C).

SEM analysis

The surface morphology of Na-Bt, PDADMAC-Bt and HDTMAB-Bt is shown in Figure 3 (a, b and, c) respectively. In the SEM images of Na-Bt (Fig. 3a) some phase separations are observed as a heterogeneous surface morphology. As can be seen, Na-Bt have massive plates and smooth surface, which indicate that there was no basal space between silicate layers.[34,38] However, the clay treated with organic surfactant (Fig. 3 b, c) shows significant changes in the morphology. There are many small and aggregated particles and the plates become relatively flat layers. Due to increase of basal spacing in organo clays more voids are seen. For HDTMAB-Bt, the surfactant-bentonite packing density increases and the clay layers are observed clearly.

Phosphate adsorption kinetics

Kinetics study is very important to determine the adsorption process to predict the capability of adsorbent to remove the phosphate ions. All the curves have similar characters, showing an important and fast adsorption, between t = 0 and 50 min, and a slower adsorption at until equilibrium is accomplished. The maximum adsorption of phosphate ions onto Na-Bt, PDADMAC-Bt and, HDTMAB-Bt samples is observed at 200, 120 and, 110 min, which is fixed as the equilibrium contact time (Fig. 4).

From Fig. 4, it can be observed that the magnitudes of phosphate ions on all surfactant modified bentonite are larger than that on Na-Bt, which can be ascribed to the hydrophobic effect and electrostatic attraction.[39] The equilibrium adsorption capacity of phosphate ions on HDTMAB-Bt is larger than that on PDADMAC-Bt, indicating Na-Bt modified by cationic surfactant with long alkyl chain is more favorable to the adsorption of phosphate ions. This phenomenon can be explained that the surface charge of adsorbent plays a significant role in the adsorption of ionisable matters. It has been pointed that larger HDTMAB-Bt was initially adsorbed by cation exchange in the interlayer, which caused extensive clay aggregation.[40,41]

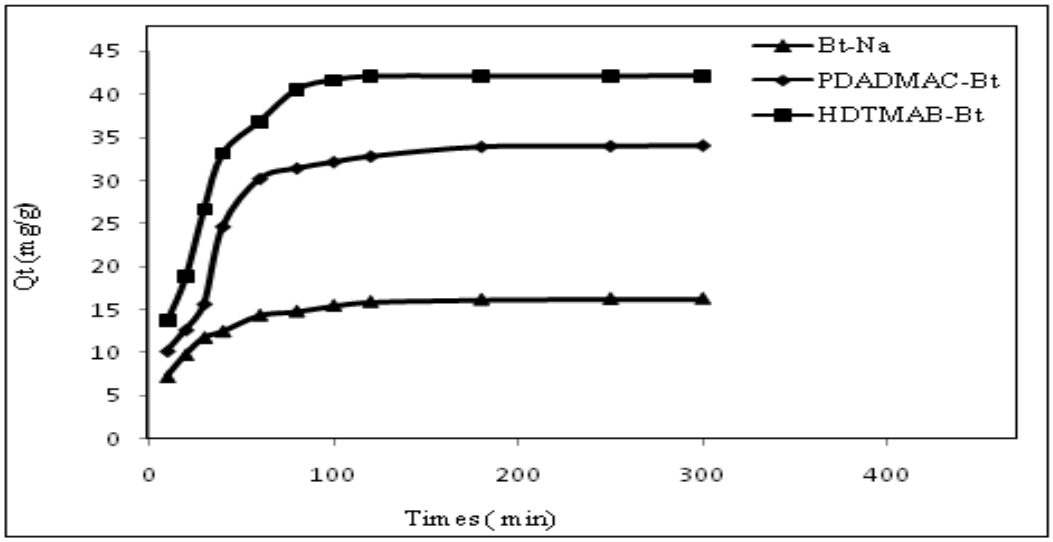

Fig. 4 – Effect of contact time on phosphate adsorption onto (A) Na-Bt, (B) PDADMAC-Bt, (C) HDTMAB-Bt. Phosphate concentration 100 mg/L, initial pH 4.5, adsorbent dose 1g/L.

To better understand the adsorption kinetics, the adsorption data of phosphate were analyzed using kinetic models such as pseudo-first order (Eq. 1), pseudo-second-order (Eq. 2), and Intraparticle diffusion (Eq. 3)

$$dq_t/dt = k_1(q_e - q_t) \quad (1)$$

$$dq_t/dt = k_2 (q_e - q_t)^2 \quad (2)$$

$$q_t = k_{int}\, t^{0,5} + C \quad (3)$$

where:
q_t (mg/g) is the adsorbed amount at time t;
q_e (mg/g) is the adsorbed amount at equilibrium;
k_1 (mg/(g min)) is the equilibrium rate constant of the pseudo-first-order kinetics model;
k_2 (mg/(g min)) is the equilibrium rate constant of the pseudo-second-order kinetics model;
k_{int} (mg/g. $min^{1/2}$) rate constant of intraparticale diffusion;
C (mg/g) intercepts.

Integrating Eq. (1) for the boundary condition t=0 to t = t and q_t =0 to $q_t = q_t$, it was rearranged to obtain a linear form:

$$Ln(q_e - q_t) = lnq_e - K_1\, t \quad (4)$$

The values of q_e, k_1 and the correlation coefficients were determined from the linear plots of $ln(q_e - q_t)$ versus t (Fig. 5), from which the kinetic data were calculated and given in Table 4.

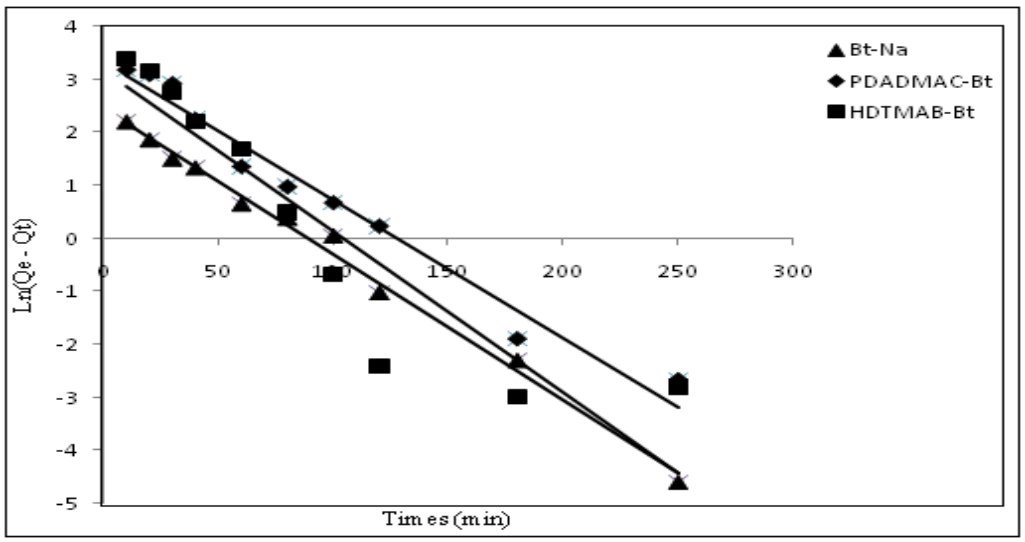

Fig. 5 – Kinetics modeling of phosphate adsorption on B t-Na (▲),PDADMAC-Bt (♦) and HDTMAB-Bt (■) using pseudo-first -order models.

Table 4

Kinetic parameters for the adsorption of phosphate onto B t-Na, PDADMAC-Bt and HDTMAB-Bt

Adsorbents	q (mg/g)	Pseudo-first-order model			Pseudo-first-order model			Intraparticale diffusion model		
		K_1 (l/g.min)	q_e (mg/g)	R^2	K_2 (l/g.min)	q_e (mg/g)	R^2	K_{int} (mg/g.min $^{1/2}$)	C (mg/g)	R^2
Bt-Na.	16.21	0.027	11.59	0.993	0.0045	17.24	0.999	0.563	8.36	0.747
PDADMAC-B_t.	34.04	0.026	27.58	0.972	0.001	38.46	0.990	1.684	10.63	0.711
HDTMAB-B_t.	42.18	0.03	23.90	0.851	0.001	45.45	0.995	1.834	17.25	0.671

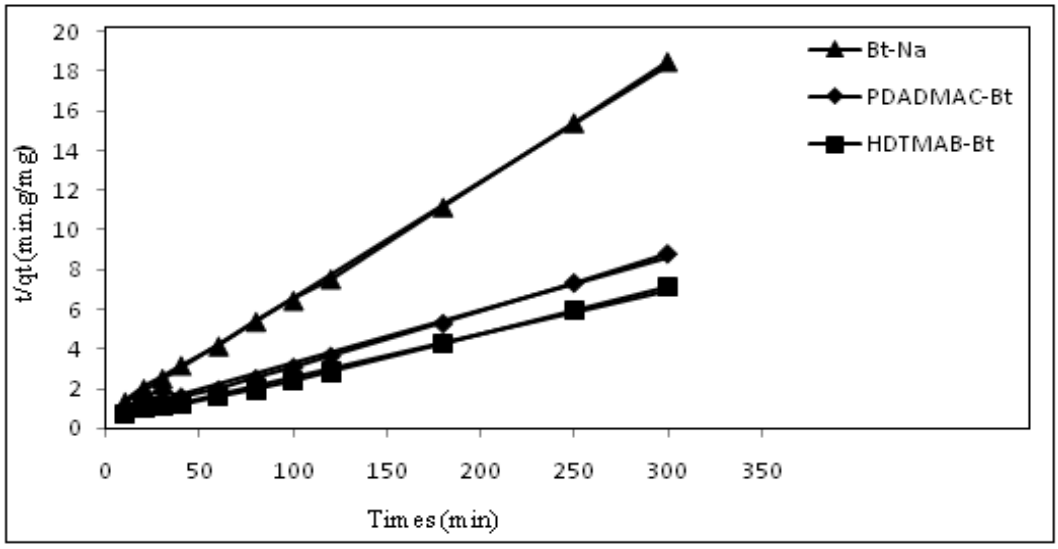

Fig. 6 – Kinetics modeling of phosphate adsorption on B t-Na (▲),PDADMAC-Bt (♦) and HDTMAB-Bt (■) using pseudo-second -order models.

Integrating Eq. (2) for the boundary condition t=0 to t = t and q_t =0 to $q_t = q_t$, it was rearranged to obtain a linear form:

$$t/q_t = 1/k_2\, q_e^2 + (1/q_e)\, t \qquad (5)$$

The values of q_e, k_2 and the correlation coefficients were determined from the linear plots of t/qt versus t (Fig. 6), from which the kinetic data were calculated and given in Table 4.

The pseudo-first-order and pseudo-second-order kinetic model cannot identify the diffusion mechanism, and then the kinetic data were analyzed by using the intraparticle diffusion model. According to this model, the plot of q_t versus the square root of time, $t^{1/2}$, for the adsorption of PO_4^{-3} onto bentonite (Fig. 7) from which the kinetic data were calculated and given in Table 4.

The correlation coefficients for the pseudo-second-order kinetic model obtained at all the studied adsorbent were found to be extremely high (>0.990) (Table 4) and the calculated q_e values obtained from this equation were also close to experimental data generally. These results indicated that the adsorption process was follow the pseudo-second-order kinetic model. The good agreement of the data with the pseudo-second-order kinetics model suggested that the chemisorption process could be a rate-limiting step.[42] The values of q_e for Na-Bt, PDADMAC-Bt and, HDTMAB-Bt were 17.24, 38.46, and 45.45 mg/g respectively, indicating an HDTMAB-Bt > PDADMAC-Bt > Na-Bt order for phosphate adsorption capacity.

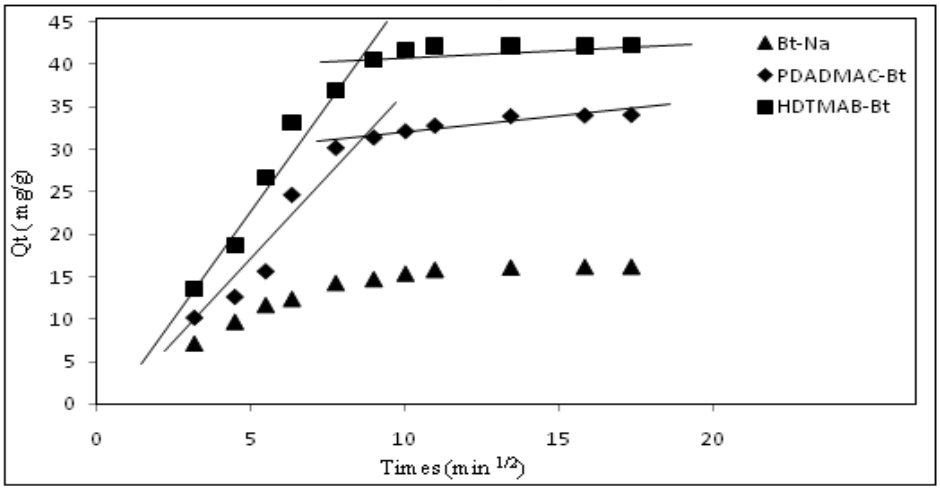

Fig. 7 – Intraparticle diffusion model for the adsorption of phosphate onto B t-Na (▲),PDADMAC-Bt (♦) and HDTMAB-Bt (■).

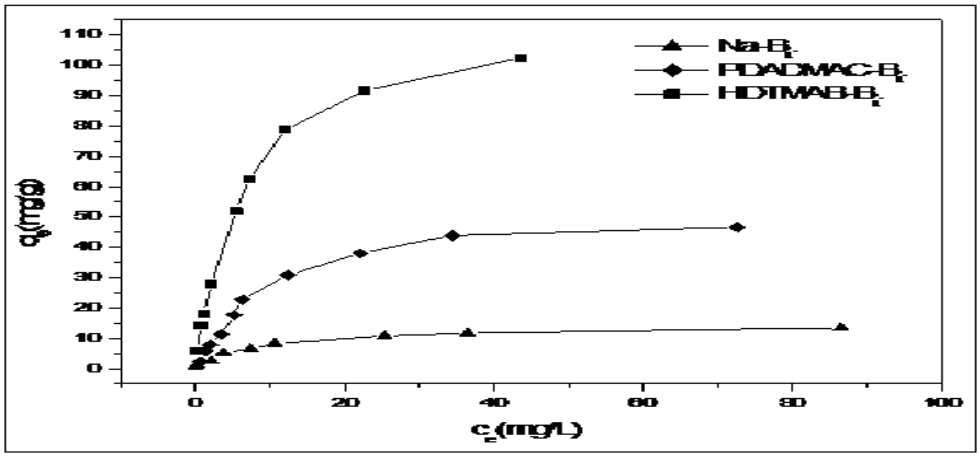

Fig. 8 – Effect of eauilibriu; concentrqtion on B t-Na (▲), PDADMAC-Bt (♦) and HDTMAB-Bt (■) At PH=4.5 and T = 25 °C.

The pseudo-first-order and pseudo-second-order kinetic model cannot identify the diffusion mechanism, and then the kinetic data were analyzed by using the intraparticle diffusion model. According to this model, the plot of uptake, qt, versus the square root of time, $t^{1/2}$, should be linear if the intraparticle diffusion is involved in the adsorption, and if these lines pass through the origin, and then intraparticle diffusion is the rate controlling step, otherwise this indicates that two or more steps occurred in the adsorption process. The plots shown in Fig. 7 presented two lines, indicating that two steps took place. As can be seen in Fig. 7, the first step described the gradual adsorption from 0 to 80 min, where intraparticle diffusion was rate-controlling. The second step was attributed to the final equilibrium stage, in which intraparticle diffusion started to slow down due to the decrease of PO_4^{-3} concentration in solution. The slope of the first step characterized the rate parameter corresponding to the intraparticle diffusion, and the intercept was proportional to the boundary layer thickness. The R^2 values of the intraparticle diffusion model were lower than that of the pseudo-second-order kinetic model, but this model indicated that the adsorption of PO_4^{-3} onto bentonite may be followed by an intraparticle diffusion model up to 80 min. This implied that although intraparticle diffusion was involved in the adsorption process, it was not the only rate-controlling step.

Sorption isotherms

The observed points of phosphate uptake capacity (qe) for the Na-Bt, PDADMAC-Bt and, HDTMAB-Bt samples in various solution phosphate concentrations (Ce) are shown in Fig. 8.

Table 5

The constants of Langmuir and Freundlich and regression coefficients for adsorption of phosphate onto Bt-Na, PDADMAC-Bt, HDTMAB-Bt

Model	Parameters	Bt-Na	PDADMAC-Bt	HDTMAB-Bt
Freundlich	K_f	2.33	3.72	5.48
	n	2.19	1.62	1.3
	R^2	0.978	0.918	0.826
Langmuir	q_{ma} (mg/g)	13.89	33.33	62.5
	K_L(L/mg)	0.233	0.016	0.273
	R^2	0.988	0.988	0996

The adsorption isotherms indicate that the uptake of phosphate increases with increasing equilibrium concentration of phosphate ions. Both figures show that all isotherms exhibited a rapid rise in the adsorption capacity with an increase in the equilibrium solution concentration, followed by a plateau at equilibrium, demonstrating typical Langmuir isotherm characteristics. In order to gain a better understanding of the adsorption mechanism, the Langmuir and Freundlich equations expressed in Eqs. (6) and (7) were used for modeling these adsorption isotherm data.

$$q_e = K_L\, q_m\, Ce) / (1 + K_L\, Ce) \quad (6)$$

$$q_e = K_f\, Ce^{1/n} \quad (7)$$

where:
Ce (mg/L) is the equilibrium adsorbate concentrations in the aqueous;
qe (mg/g) is the equilibrium adsorbate concentrations in the solid phases;
q_m (mg/g) is the maximum adsorption capacity;
K_L (L/g) is the Langmuir adsorption equilibrium constant;
K_f is the Freundlich equilibrium constant indicative of adsorption capacity;
1/n is the Freundlich adsorption constant, the reciprocal of which is indicative of adsorption intensity.

The Langmuir isotherm equation can be rearranged to the linear form given below:

$$C_e /q_e = Ce /q_m + 1 /K_L\, q_m \quad (9)$$

q_m and K_L can be calculated from the slope and intercept of the linear plot with C_e /q_e versus Ce.

Based on the Langmuir equation, a dimensionless constant i.e., termed separation factor (R_L, also termed equilibrium parameter) is commonly used to predict whether a sorption system is favorable or unfavorable (Bulut *et al.*, 2008). RL can be expressed using the following Eq. (10):

$$RL = 1/(1+ K_L\, C_0) \quad (10)$$

The Langmuir equation is applicable to homogeneous sorption, where the sorption of each sorbate molecule onto the surface has equal sorption activation energy[35]

The Freundlich isotherm equation can be rearranged to the linear form given below:

$$Logq_e = LogK_f + 1/n\ logC_e \quad (11)$$

K_f and n can be calculated from the slope and intercept of the linear plot with $Logq_e$ versus $logC_e$.

The values of n indicate the degree of non lineaire between phosphate solution concentration and adsorption (Kundu and Gupta, 2006):
n<1 adsorption process is chemical;
n=1 linear adsorption is linear;
n>1 adsorption is favorable physical.

The Freundlich equation is employed to describe heterogeneous systems and reversible adsorption and is not restricted to the formation of monolayers.[36]

Table 5 summarizes the constants of the Langmuir and Freundlich adsorption isotherms of phosphate adsorption onto the three bentonites samples. The maximum adsorption capacities (q_m) calculated from the Langmuir model were 13.89, 52.63, and 62.5 mg/g for Bt-Na, PDADMAC-Bt and, HDTMAB-Bt respectively. For both Bt-Na, PDADMAC-Bt and, HDTMAB-Bt, the Langmuir isotherm model gave a better fit than the Freundlich isotherm model as shown by the higher R^2 values. Similar results have been reported for the adsorption of phosphate by hybrid surfactant akaganéite.[34] From Table 5, the calculated q_m and K_f followed the order of HDTMAB-Bt > PDADMAC-Bt > Bt-Na, which indicate the capacity of phosphate adsorption. In addition, HDTMAB-Bt had a high K_L value, which is related to binding energy of phosphate adsorption, implying that phosphate adsorbed on the HDTMAB-Bt was more difficult to be desorbed and could be held longer. Similar results regarding phosphate sorption capacity was obtained from Freundlich model (K_F value). The parameters n from the Freundlich equation and K_L from the Langmuir model were not directly comparable. The K_L in the Langmuir model measures the

affinity of the adsorbent for the solute (a lower value for $K_L < 1$ indicates adsorption process is chemical). On the other hand, the constant n refers to the interaction between exchange sites in the adsorbent and phosphate ions. A high value for n> 1 indicates favorable physical adsorption.

MATERIALS AND METHODS

Preparation of Na-Bentonite

Bentonite used in this investigation was purchased from National Company for Geological and Mining and it was collected from Hammam Boughrara, west of Algiers. The chemical constituents of the bentonite are illustrated in Table 1. Bentonite was purified to remove carbonates, calcites, iron hydroxide and organic metals, and dispersed in distilled water. Particles with diameter <2 μm were obtained by sedimentation and saturated with Na^+ by keeping the clay suspension in 1M NaCl for 24 h. After that, the sample was washed with purified water to remove the excess of Na^+. Finally, the suspension was centrifuged, the supernatant removed and the solid was dried at 60 °C, and stored in tightly closed plastic bottles for use in the experiments. This sodium-exchanged clay will be called Na-Bt.

Cationic polymers

The polymer poly-diallil-dimethyl-ammonium-chloride (PDADMAC) was purchased from Merck, with has the viscosity 300 cP, concentration 20 wt. % in H_2O, density 1.04 g/mL and the formula $(C_8H_{16}ClN)_n$. The hexadecyltrimethylammonium bromide (HDTMAB) salt of formula $CH_3(CH_2)_{15}N(Br)(CH_3)$ was purchased from Aldrich. All chemicals used in the analyses were of analytical grade.

Organo-clay bentonite

The required weight of electrolyte was mixed with demonized water to give 100 mL of 5% of surfactant solution. This solution was then added to a suspension of NaBt containing 20 g oven-dried equivalent of clay that had been stirred into 100 ml of deionized water in a container in order to satisfy CEC 89.81 meq/100 g of bentonite. The mixture was subjected to a chemical stirring at 70 °C for 2 hours to obtain the complex with suitable surfactant content. Bentonite was then separated from solution via filtration, washed three times with distilled water, oven dried at 105 °C.[21,22] The bentonite grafted with PDADMAC and with HDTMAB is designated as (PDADMAC-Bt) and (HDTMAB-Bt) respectively.

Phosphate aqueous solution

The phosphate (PO_4^{3-}) stock solution of 50 mg/L was prepared by dissolving 0.2197 g potassium dihydrogen orthophosphate (KH_2PO_4) powders (analytical reagent grade) in 1 L deionized water. Phosphate solutions of desired concentrations were obtained by dilution in 0.01 mol/L KCl solution (KCl as background electrolyte).

Methods of characterization

The elemental analysis of samples was conducted by X-ray fluorescence (XRF) on PHILIPS PW 1,480 spectrometer that used a wave length dispersive technical. The X-ray diffraction (XRD) data of natural and acid activated samples were obtained by a SIEMENS D 5000 difractometer equipped with graphic monochromator CuKα radiation and a fixed power source (40 KV, 40 mA) was used; the scan rat was 0.5º $(2\theta)min^{-1}$. Before chemical analysis, each sample dried at 105 °C for 4 hours was heated 1000 °C for 2 hours, and the decrease in mass was taken as the loss on ignition (LOI).

The FT-IR spectra were recorded with FT-IR Spectrophotometer Model 4400 (Shimadzu Corporation, Japan) with 1 cm^{-1} resolution and in the range 400 – 4,000cm^{-1}. Solid clay was mixed with KBr in 1:10 ratio. The mixture was grinded to very fine powder. The fine powder was pressed under 10 ton pressure into pellet. The Infrared spectra were obtained from solid samples and KBr pellets.

Scanning electron microscopy (SEM) of the solid catalysts was carried out at 15 kv using a Jeol scanning electron microscope, model JSM-630LV. Each sample specimen was deposited on an aluminium stub and gold sputtered prior to analysis by SEM.

Phosphate was analyzed by the molybdenum blue method.[23] Molybdenum acid ammonium solution, 2.0 ml, and an L-ascorbic acid solution, 1.0 mL, were added to the sample solution. After 15 min, the absorbance at a wavelength of 700 nm with UV–visible recording spectrophotometer (UVmini-1240 SHIMADZU) using 10 mm

matched quartz cells. The values for initial phosphate concentration (C_0) and final phosphate concentration (Ce) were used to calculate the uptake capacity (qe) as the amount of phosphate sorbed at equilibrium per amount of powdered fiber sample (mg/g). Analyses were carried out in triplicate.

Phosphate adsorption kinetics

Phosphate adsorption kinetics was conducted using a horizontal thermostated shaker (SPH-103B, Shanghai Shiping Laboratory Equipment Co., Ltd.) operated at 300 rpm, at room temperature (25 °C) and an initial PO_4^{-3} concentration in the suspension was 100 mg/L. Portions of 0.25 g bentonite were placed into 250 ml Erlenmeyer flasks, and placed it in a temperature controlled shaker to enhance reaction equilibrium. This adsorbate-adsorbent ratio was selected to ensure that residual phosphate concentrations were above detectable levels during the experiments. The pH of the solution was maintained at 7.5^{20}. The samples were taken in triplicates at the intervals of 0, 10, 20, 25, 30, 40, 60, 80, 90, 120, 180, 250 and 300 min. The withdrawn samples were filtered through a 0.45 μm filter.

Phosphate adsorption isotherms

The isotherm studies were conducted using a horizontal thermostated shaker (SPH-103B, Shanghai Shiping Laboratory Equipment Co., Ltd.) operated at 300 rpm, at room temperature (25 °C) for 24 h. The 0.25 g of adsorbent solids was added into 250 mL phosphate solution, with pH preadjusted to 7.5, using 10 mM NaOH solutions. The initial phosphate concentrations of the samples ranged from 0.5 to 100 mg L^{-1}. After 24 h, the samples were filtered through a 0.45 μm filter and the phosphate concentrations in the filtrates were measured using the molybdenum blue method. The data of the triplicate analyses were then averaged.

CONCLUSION

The sodic bentonite and organo-modified were tested to remove phosphate ions from aqueous solution. The surface structure of the materials was investigated. The change of surface properties from hydrophilic to hydrophobic and increased anions adsorption capacity are two positive points of using organic surfactant as sodic bentonite modifier. Results reveal that modified bentonite with Hexadecyltrimethylammonium bromide (HDTMAB-Bt) is the most efficient absorbent for phosphate ions. The pseudo-second-order model accurately described the phosphate adsorption kinetics for the three prepared adsorbent. The results show that the organo-modified bentonite had faster kinetics and higher adsorption capacities than the sodic bentonite sample. The obtained results promoted the use of the prepared organo-modified bentonite as potentially attractive adsorbents for the removal of phosphate from aqueous solution.

ABBREVIATIONS

HDTMAB-Bt = HexaDecylTrimethylAmmoniumBromide-Bentonite.
PDADMAC-Bt=PolyDiethylDialliltetraAmmoniumChloride-Bentonite.

REFERENCES

1. P. Kofinas and D. R. Kiossis, *Environ. Sci. Technol.*, **2003**, *37*, 423.
2. H. D. Ruan and R. J. Gilkes, *J. Environ. and Quality.*, **2000**, *29*, 1875.
3. B. Grzmil and J. Wronkowski, *Desalination*, **2006**, *189*, 261.
4. D. Jenkins, J. F. Ferguson and A. B. Menar, *Water Research*, **1971**, *5*, 369.
5. E. Arvin, *Rev. Water Sci. Technol.*, **1983**, *15*, 43.
6. J. Li, H. X. Ren, Liu Q. Wang and Q. Xie, *Pollution Engineering*, **2005**, *37*, 14.
7. R. Camarillo, I. Asencio and J. Rincón, *Desalination and water treatment*, **2009**, *6*, 211.
8. L. Ruixia, G. Jinlong and T. J. Hongxiao, *J. Colloid Interface Sci.*, **2002**, *248*, 268.
9. T. Nir, E. Arkhangelsky, I. Levitsky and V. Gitis, *Desalination and water treatment*, **2009**, *8*, 24.
10. R. Chitrakar, S. Tezuka, A. Sonoda, K. Sakane, K. Oi and T. Hirotsu, *J. Colloid Interface Sci.*, **2006**, *297*, 426.
11. A. Gieseke, P. Arnz, R. Amann and A. Schramm, *Water Research*, **2002**, *36*, 501.
12. Y. Kim and J. Yi, *J. Ind. Eng. Chem.*, **2004**, *10*, 41.
13. L. W. Shan, Y. C. Chia, Y. T. Min, B. L. Ren, T.-W. Chang and J.-H. Chena, *J. Hazardous Mater.*, **2007**, *147*, 205.
14. N. Yilmaz, H. Yilmaz and S. Yapar, *Energy Sources* (Part A), **2007**, *29*, 67.
15. N.Yılmaz and S. Yapar, *Appl. Clay Sci.*, **2004**, *27*, 223.
16. T. O. Salawudeen, A. M. Suleyman, F. A. Ma'an, Y. Q. Isam., H. S. Qassim and Y. Faridah, *Kuliyah of Engineering Research Innovation and Exhibition*, IIUM, Malaysia, 2009, p. 32.
17. Y.Xi, M. Mallavarapu and R. Naidu, *Appl. Clay Sci.*, **2010**, *48*, 92.
18. A. H. Gemeay, A. S. El-Sherbiny and A. B. Zaki, *J. Colloid Interface Sci.*, **2002**, *245*, 116.

19. E. Orucoglu and S. Haciyakupoglu, *Kibited I*, **2010**, *4*, 21.
20. S.-L. Wang, C.-Y. Chenga, Y.-M. Tzoua, R.-B. Liaw, T.-W. Changd and J.-H. Chena, *J. Hazardous Mater*., **2007**, *147*, 205.
21. W. X. Liu, V. H. Ni and H. N. Xiao, *Trans. China Pulp Paper*, **2005**, *169*, 20.
22. L. R. Han, A. H. Lu and C. X. Chen, *Acta Petero. Mineral.*, **2001**, *20*, 455.
23. D. Momento, "Technique de l'eau", 10 eddition, Lavoisier, 2005.
24. N. Makhokhi, "Modification of the raw bentonite by several organic salts– applications for oils decoloration and adsorption of textiles dyes", PhD thesis, University of Telemcen, Algeria, 2008.
25. G. Lagaly and A.Weiss, *Kolloid Zeitschrift & Zeitschrift für Polymere*, **1970**, *243*, 48.
26. G. Lagaly, M. Ogawa, I. Dekany, F. Bergaya, B. K. G. Theng and G. Lagaly, "Clay mineral organic interactions", Handbook of clay science, Developments in Clay Science., vol. 1, Elsevier, Amsterdam, 2006, p. 309–377.
27. S. Y. Lee, and J. K. Soo, *Colloids and Surfaces A: Physicochem. and Engineer. for Aspects*., **2002**, *211*, 19.
28. S. Y. Lee, J. C. Wrin, P. S. Hahn, M. Lee, Y. B. Lee and K. J. Kim, *Appl. Clay Sci.*, **2005**, *30*, 174.
29. Y. Xi, M. Mallavarapu and R. Naidu, *Appl. Clay Sci.*, **2010**, *48*, 92.
30. L. Zhu and R. Zhu, *Sep. Purif. Technol.*, **2007**, *54*, 71.
31. H. Zaghouane-Boudiaf and M.Boutahala, *Advanced Powder Techol.*, **2011**, *22*, 735.
32. S. S. Bhattacharya and A. Mandot, *Research J. Engineering Sci.*, **2014**, *3*, 10-16.
33. U. O.Aroke and U. A. El-Nafaty, *Int. J. Emergency Technol. Advanced Engineering*, **2014,** *4*, 4.
34. Y. H. Zhang and K. C. Gong, *Bull. China Ceramic Soc.*, **1998**, *1*, 24.
35. D. G. Lopeza, I. Gobernado-Mitre, J. F. Fernandez, J. C. Merino and J. M. Pastor, *Polymer*., **2005**, *46*, 2758.
36. Y. Jui-Ming, H. Hsiu-Yin, C. Chi-Lun, S. Wen-Fen and Y. Yuan-Hsiang, *Surf. Coat. Technology*., **2006,** *200*, 2753.
37. C. Daimei, C. Jian, X. Luan, J. Haipeng and X. Zhiguo, *Chem. Engineering J*., **2011**, *171*, 1150.
38. S. Xu and S. A. Boyd, *Environ. Sci. Technol.*, **1995**, *29*, 3022.
39. Y. S. Ho and G. McKay, *Biochem.*, **1999**, *34*, 451.
40. S. Gammoudi, N. Frini-Srasra and E. Srasra, *Appl. Clay Sci.*, **2012**, *69*, 99.
41. L. Zatta, L. P. Ramos and F. Wypych, *Appl. Clay Sci*., **2013**, *80–81*, 236.
42. M. Kozak, L. Domka, *J. Phys. Chem. Solids*, **2004,** *65*, 441.